

E15-2001-188

O.Yu.Smirnov, O.A.Zaimidoroga, A.V.Derbin \*

SEARCH FOR THE SOLAR  $pp$ -NEUTRINOS  
WITH AN UPGRADE OF CTF DETECTOR

Submitted to «Ядерная физика»

---

\*St. Petersburg Nuclear Physics Institute, Gatchina, Russia

# 1 Introduction

Present information on the solar neutrinos spectrum are based on the very tail of the total neutrino flux (about 0.2%). Meanwhile, the spectrometry of the solar neutrino spectrum is the main source of information on the new neutrino physics. The pp neutrinos measurement is a critical test of stellar evolution theory and of neutrino oscillation solutions. A discussion of the physics potential of the pp solar neutrino flux can be found in [1] and [2]. The low energy part of the spectrum, and in particular pp-neutrino flux, has not been measured directly until now. A number of projects aiming to build pp-neutrino spectrometers are in the initial stages of the development. The principal characteristics of the existing proposals are shown in table 1. The existing radiochemical experiments are not cited in the table.

## 2 Borexino and its Counting Test Facility

Borexino, a real-time detector for low energy neutrino spectroscopy, is near completion in the underground laboratory at Gran Sasso (see recent [17] and references therein). The main goal of the detector is the direct measurement of the flux of  ${}^7\text{Be}$  solar neutrinos of all flavours via neutrino-electron scattering in an ultra-pure liquid scintillator. Borexino will also address several other frontier questions in particle physics, astrophysics and geophysics.

The CTF was constructed and installed in Hall C of the Gran Sasso Laboratory. The main goal of the CTF was a demonstration of the possibility of liquid scintillator purification on the scale of several tons. Although the CTF is a large-scale detector (4 tons of liquid scintillator), its size is nonetheless modest in comparison to Borexino (300 tons). A mass in the 4 ton range was set by the need to make the prevailing scintillator radioimpurities measurable via delayed coincidence of tagged events<sup>1</sup>, while a water shield thickness of approximately 4.5 m was needed in order to suppress the external radiation. The primary goal of the CTF was to develop a solution directly applicable to operational issues for Borexino; in the future there will be also the long-range goal of performing quality control during Borexino operations. Detailed reports on the CTF have been published [13],[15],[14]. As a simplified scaled version of the Borexino detector, a volume of liquid scintillator is

---

<sup>1</sup>Key components in the decay chains of U/Th and in the  $\beta$ -decay of  ${}^{85}\text{Kr}$  are emitted as time-correlated coincidence pairs which can be tagged with high specificity.

Project (reference)	Method	Threshold [keV]	Resolution	Mass [t]	Reaction	pp events [ $d^{-1}$ ]
LENS [3]	$^{176}\text{Yb}$ , LS	301 ( $\nu$ )	7% @ 1 MeV	20 (8% nat $^{176}\text{Yb}$ )	$^{176}\text{Yb} + \nu_e \rightarrow$ $^{176}\text{Lu} + e^-$	0.5
INDIUM [4]	$^{115}\text{In}$ LS	118 ( $\nu$ )	5-10% @1 MeV	4	$^{115}\text{In} + \nu_e \rightarrow$ $^{115}\text{Sn}^*(613) + e^-$	1.0
GENIUS [5]	$^{76}\text{Ge}$ scatt	11 ( $e^-$ ) 59 ( $\nu$ )	0.3% @ 300 keV	1 10	$\nu + e^- \rightarrow$ $\nu + e^-$	1.8 18
HERON [7]	superfluid $^4\text{He}$ rotons/phonons+uv	50 ( $e^-$ ) 141 ( $\nu$ )	8.3% @364 keV	10	$\nu + e^- \rightarrow$ $\nu + e^-$	14
XMASS [9]	liquid Xe scintill	50 ( $e^-$ ) 141 ( $\nu$ )	17.5% @ 100 keV	10	$\nu + e^- \rightarrow$ $\nu + e^-$	14
HELLAZ [10]	He (5 atm), TPC	100 ( $e^-$ ) 217 ( $\nu$ )	6% @800 keV	2000 $m^3$	$\nu + e^- \rightarrow$ $\nu + e^-$	7
MOON [6]	drift chambers	168 ( $\nu$ )	12.4% FWHH @ 1 MeV	3.3	$\nu_e + ^{100}\text{Mo} \rightarrow$ $^{100}\text{Tc} + e^-$	1.1
MUNU [8]	TPC, $CF_4$ direction	100 ( $e^-$ ) 217 ( $\nu$ )	16% FWHH @ 1 MeV	0.74 (200 $m^3$ )	$\nu + e^- \rightarrow$ $\nu + e^-$	0.5
NEON [11]	He, Ne scintill	20 ( $e^-$ ) 82 ( $\nu$ )	16% FWHH @ 100 keV	10	$\nu + e^- \rightarrow$ $\nu + e^-$	18
this	LS	170 ( $e^-$ ) 310 ( $\nu$ )	10.5 keV @ 200 keV	10	$\nu + e^- \rightarrow$ $\nu + e^-$	1.8

Table 1: Key characteristics of the solar neutrino projects sensitive to the pp-neutrino.

contained in a 2 m diameter transparent inner nylon vessel mounted at the center of an open structure that supports 100 phototubes (PMT) [18] which detect the scintillation signals. The whole system is placed within a cylindrical tank (11m in diameter and 10m height) that contains 1000 tons ultra-pure water, which provides a shielding against neutrons originating from the rock and against external  $\gamma$ -rays from PMT's and other construction materials. The scintillator used for the major part of the testing in the CTF is pseudocumene (PC,  $C_9H_{12}$ ). The upgrade of the CTF-I detector (CTF-II) was operating with an alternate liquid scintillator (LS) solvent, phenylxylylethane (PXE,  $C_{16}H_{18}$ ). The scintillator is carefully purified to ensure the  $^{238}U$  and  $^{232}Th$  in it are less than some units  $10^{-16}$  g/g. The PMT's are 8 inch ETL 9351 tubes made of low radioactivity glass and characterized by high quantum efficiency (26% at 420 nm), limited transit time spread (1 ns) and good pulse height resolution for single photoelectron pulses (Peak/Valley = 2.5). The number of photoelectrons registered by one PMT for the 1 MeV energy deposit at the detector's center is about 3.5 for the PXE.

### 3 Upgrade of the CTF detector

The geometry of the proposed upgrade is presented in the fig.1 in comparison with Borexino and CTF. The inner vessel is the transparent spherical nylon bag with a radius of 240 cm, containing 50 tons of ultrapure pseudocumene ( $C_9H_{12}$ ) with 1.5 g/g of PPO. The active shielding is provided by 100 cm of the outer layer of pseudocumene (PC). The 800 PMTs are mounted on the open structure at the distance 440 cm from the detector's center (distance is counted from the PMT photocathode). The comparison of the geometrical parameters of Borexino, CTF and its upgrade is presented in the table.2.

The choice of the geometry is motivated by the following reasons:

- the detector should fit in the existing CTF external tank, which is 10 meters height and 11 meters in diameter;
- the light registration system should provide maximum possible geometrical coverage with a minimal number of PMTs required;
- the active shielding of the fiducial volume is provided by at least 100 cm of PC;

- the passive shielding from the gammas originated from PMT impurities is provided by 200 cm of ultrapure water;
- fiducial volume of the detector should be of the order of 10 tons;
- the inner vessel size should be as small as possible in order to avoid the loss of light in the scintillator and to provide better detector uniformity;
- to lower the detector's threshold ( $< 35$  keV) in order to acquire the  $^{14}\text{C}$  spectrum shape without deformations caused by the threshold effects.

The Borexino- sized detector is unfavourable solution because of the huge number of the PMTs necessary to provide  $4\pi$  coverage. The big inner vessel volume in turn decreases the amount of the light escaping from the interior part of the detector. The spatial reconstruction of the lower energy events is complicated because of the multiple absorption and reemission of the light on the way to the PMT with a characteristic length of 1 m [14].

The beta decays of  $^{14}\text{C}$  in the liquid organic scintillator sets a lower threshold on the detector sensitivity. The content of the  $^{14}\text{C}$  in pseudocumene used in the CTF detector was at the level of  $2 \times 10^{-18}$  g/g with respect to the  $^{12}\text{C}$  content. Though the end point of the  $^{14}\text{C}$  beta- decay is only 156 keV, the energy resolution of the CTF (and Borexino) is not good enough at this energy in order to set threshold lower than 250 keV. We suggest to use additional PMTs supplied with hexagonal light concentrators in order to provide  $4\pi$  coverage, in comparison to 21% for CTF and 30% for Borexino. Additional energy resolution improvement (about 15%) in the low energy region can be achieved by using an energy reconstruction technique discussed in [21].

We considered the contamination of the pseudocumene with the radionuclides of the  $U - Th$  chain and with  $^{40}\text{K}$  on the level envisaged for the Borexino scintillator. These levels were achieved on the CTF. In such a way we expect about 2 events/day due to the internal background in 10 tons of scintillator. Due to the better energy resolution there is possibility to recognize the signals of the unidentified alpha-particles in the region between 350 and 500 keV that give about 30% of the total background in the Borexino "neutrino window" (250-700 keV). The better energy and spatial resolutions will permit to improve the  $\alpha/\beta$  discrimination capability of the CTF upgrade in comparison to CTF. The decrease of the threshold energy will

allow as well to improve the delayed coincidence (DC) discrimination of the events from the radioactive chains.

The outer layer of active volume (100 cm) is used as an active shield against the gamma's (mainly from the  $^{40}\text{K}$  contained in the PMT glass bulbs). The additional passive shielding with 200 cm of ultrapure water is considered in the present design.

Detector should be supplied with an external muon veto system. The muon veto system consisting of about 50 additional PMTs can be mounted on the top and on the bottom of the cylindrical external tank. The muon recognition efficiency should be at the level of 99.99% in order to guarantee missed muons count  $< 0.1$  per day.

Parameter	CTF	Borexino	CTF upgrade
Geometrical coverage	21%	30%	$\cong 100\%$
Light yield (p.e./MeV)	360	400	1800
Light yield per PMT for the event at the detector's center $\mu_0$ [p.e./PMT/1 MeV]	3.6	0.25	2.25
Energy resolution @ 200 keV [keV] ( $\sim \frac{1}{\sqrt{\text{Lightyield}}}$ )	27	26	10.5
Threshold (keV)	250	250	170
Muon veto PMTs	16	200	50
PMTs number	100	2200	800
Total natural K content in the PMTs [g]	8	176	64
Distance between the PMTs and detector's center [cm]	330	675	440
Spatial resolution @ 200 keV [cm] ( $\sim \langle \frac{1}{\sqrt{N_{hit}}} \rangle \cong \frac{1}{\sqrt{N_{PM}(1-e^{-0.2\mu_0})}}$ )	20	45	8

Table 2: Comparison of the main features of the CTF, Borexino and proposed upgrade of the CTF detector

## 4 Detector's energy resolution

A detailed analysis of the large volume liquid scintillator detector energy resolution can be found in [20] and [21]. We give here a brief overview of the main results because of the importance for further discussion. Taking into account the dependence of the registered charge on energy one can write for the CTF charge resolution<sup>2</sup>:

<sup>2</sup>This is the case when no energy reconstruction is performed and the energy is defined by dividing the total registered charge by the p.e. yield A:  $E = \frac{Q}{A}$ .

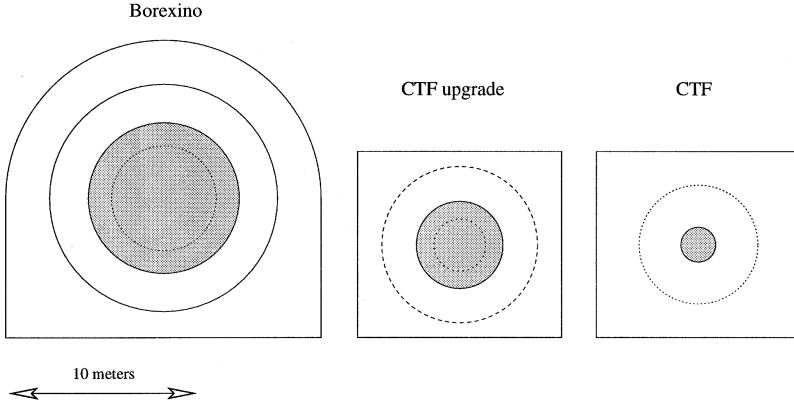


Figure 1: Comparison of the geometry of the Borexino, CTF and proposed upgrade of the CTF detector. The inner vessel with scintillator is shown with a gray colour. The dashed line inside the inner vessel defines the fiducial volume, outer layer is protecting the fiducial volume from the external gammas. PMTs are uniformly distributed by the surface shown with a solid line on the Borexino drawing and with a dashed line on the two others.

$$\frac{\sigma_Q}{Q} = \sqrt{\frac{1 + \bar{v}_1}{A \cdot E \cdot f(k_B, E) \cdot v_f} + v(p)}, \quad (1)$$

where

$\bar{v}_1 = \frac{1}{N_{PM}} \sum_{i=1}^{N_{PM}} s_i v_{1_i}$  is the relative variance of the PMT single photoelectron charge spectrum ( $v_{1_i}$ ) averaged over all CTF PMTs ( $N_{PM}$ ), taking into account the  $i$ -th PMT relative sensitivity  $s_i$ ;

$A$  is scintillator light yield measured in photoelectrons per MeV;

$f(k_B, E)$  is the function taking into account suppression of the light yield at the low energies, so called ionization quenching; the function has been studied in [22];

$v(p)$  is the parameter which takes into account the variance of the signal for the source uniformly distributed over the detector's volume. Because of the detector's spherical symmetry one can describe the dependence of the registered charge on

the distance from the event to the detector's center  $\mathbf{r}$  with a function of  $\mathbf{r}$ ,  $Q(r) = Q_0 f_R(r)$ , where  $Q_0$  is the charge collected for an event of the same energy occurring at the detector's center. The  $v(p)$  parameter is the relative variance of the  $f_R(r)$  function over the detector volume:

$$v(p) \equiv \frac{\langle f_R^2(r) \rangle_V}{\langle f_R(r) \rangle_V^2} - 1; \quad (2)$$

$v_f$  is volume factor, coming from the averaging of the signals over the CTF volume,  $v_f \equiv \frac{\langle Q(r) \rangle_V}{Q_0}$ .

For the details of the meaning of the parameters see [20] and [21]. For the signal calculation we used the following parameters:  $A=1800$  p.e./MeV,  $v_1 = 0$ ,  $v_f = 1$ ,  $v(p)=2.3 \times 10^{-3}$ ,  $k_B = 0.0167$ .

The signal  $S(Q)$  registered by the detector is the convolution of the "pure" signal spectrum  $S_0(Q)$  with the detector's resolution:

$$S(Q) = N_0 \int S_0(E(Q')) \frac{dE}{dQ} Res(Q, Q') dQ' \quad (3)$$

where  $Res(Q, Q') = \frac{1}{\sqrt{2\pi\sigma_Q}} e^{-\frac{1}{2}(\frac{Q-Q'}{\sigma_Q})^2}$  is the detector response function, and  $\sigma_Q$  is defined by (1).

## 5 Detector's spatial resolution

The spatial resolution of the detector is proportional to the mean of the inverse number of PMTs hit in the event:

$$\sigma_{x,y,z} = \sigma_0 \left\langle \frac{1}{\sqrt{N_{hit}}} \right\rangle \cong \frac{\sigma_0}{\sqrt{N_{PM}(1 - e^{-\mu_0 E F(T_{cut}, \mu)})}}, \quad (4)$$

where  $\mu_0$  is the mean p.e. number registered for an event of 1 MeV at the detector's center,  $N_{PM}$  is number of PMTs of the detector,  $F(T, \mu) = \int_{T_{min}}^T \rho(t, \mu)$  is the part of the p.d.f. of the photoelectron registering at time  $t$ , that has been taken into account in the reconstruction algorithm.

The results of the estimation of the spatial resolution for 3 detector geometries (CTF, Borexino and CTF upgrade) are shown in fig.2. The  $\sigma_0$  value for the CTF detector is  $\sigma_0(1MeV) = 10cm$  (measured value, [13]), for the Borexino we used the



results of MC simulations giving  $\sigma_0(1\text{MeV}) = 10\text{cm}$  ([17]), and  $\sigma_0 = 3.5\text{cm}$  for the CTF upgrade was obtained scaling the CTF result by the factor  $\sqrt{\frac{N_{PM}(\text{Upgrade})}{N_{PM}(\text{CTF})}} = \sqrt{8}$ .

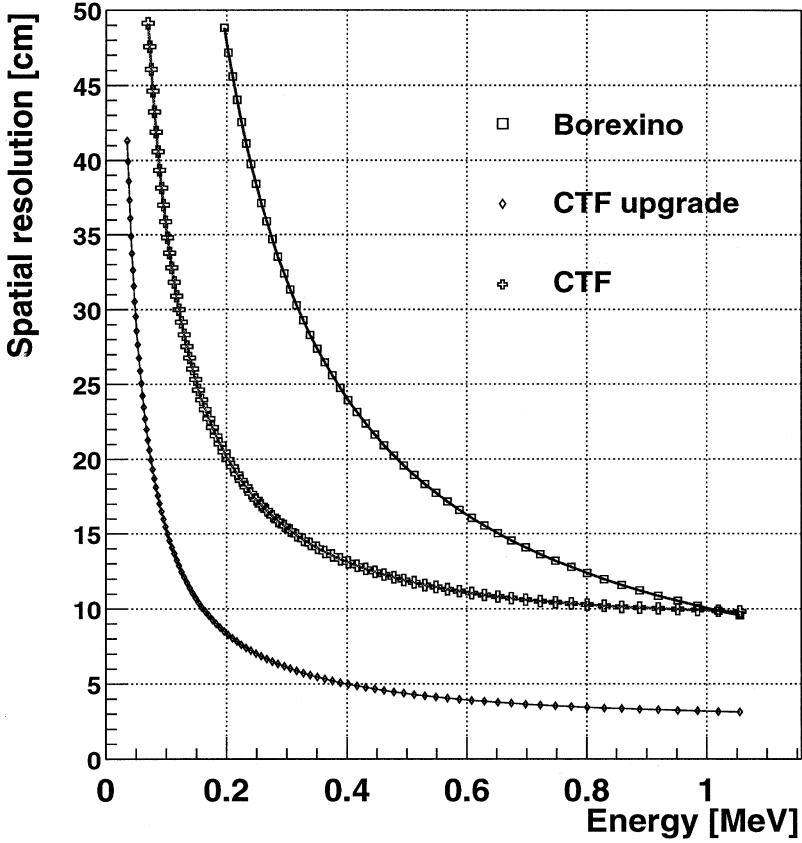


Figure 2: Spatial resolution of 3 detectors as a function of event energy.

## 6 Backgrounds

The sensitivity of the detector depends on the presence of the background in the 170-250 keV energy window. As in CTF or Borexino ([13],[17]) the main sources of background are

- internal background, including  $^{14}\text{C}$  beta- decay counts in the neutrino window;
- background from the radon dissolved in the buffer ;
- external gamma background;
- cosmic ray background.

In the following subsections we give an estimate of the background contribution from each source.

### 6.1 Internal background from the metallic ions

The contamination of the scintillator with natural radioactive isotopes gives a total rate of 2400 events/year with the following assumptions:

- secular equilibrium of the radioactive elements in the decay chains;
- the  $^{238}\text{U}$ ,  $^{232}\text{Th}$  and  $K_{nat}$  (natural potassium) content in the scintillator is  $10^{-16}$  g/g;
- a 90% capability to reject alphas ( $\alpha/\beta$ - discrimination technique based on the different shape of the detector response to  $\alpha$  and  $\beta$ );
- 95% rejection efficiency of the delayed coincidence method based on the tagging of the  $^{214}\text{Bi} - ^{214}\text{Po}$  decay chain;
- 95% efficiency of the statistical subtraction method based on the deducing the isotopes in the chain preceding the Bi-Po coincidence

A more complete discussion of the background reduction techniques can be found in [12]. The excellent detector's resolution can improve the efficiency of the all techniques.

Only 140 events of the total amount falls into the 170-250 keV energy window.

## 6.2 $^{14}\text{C}$ background

### 6.2.1 $^{14}\text{C}$ spectrum

The major part of the CTF background in the energy region up to 200 keV is induced by  $\beta$ -activity of  $^{14}\text{C}$ . The  $\beta$ -decay of  $^{14}\text{C}$  is an allowed ground-state to ground-state ( $0^+ \rightarrow 1^+$ ) Gamow-Teller transition with an endpoint energy of  $E_0 = 156$  keV and half life of 5730 yr. The beta energy spectrum with a massless neutrino can be written in the form [29]:

$$dN(E) \sim F(Z, E)C(E)pE(Q - E)^2dE \quad (5)$$

where

$\mathbf{E}$  and  $\mathbf{P}$  are the total electron energy and momentum;

$F(\mathbf{E}, \mathbf{Z})$  is the Fermi function with correction of screening by atomic electrons;

$C(\mathbf{E})$  contains departures from allowed shape.

For  $F(\mathbf{E}, \mathbf{Z})$  we used the function from [30] which agrees with tabulated values of the relativistic calculation [31]. A screening correction has been made using Rose's method [32] with screening potential  $V_0 = 495$  eV. The  $^{14}\text{C}$  spectrum shape factor can be parametrized as  $C(E) = 1 + \alpha E$ . In our calculation we used the value  $\alpha = -0.72$  [16].

The total amount in the 170-250 keV window with the energy resolution corresponding to 1800 p.e./MeV is 3485 events/year if the  $^{14}\text{C}$  content is  $2 \times 10^{-18}$  g/g. This is the content achieved with the CTF-I setup [16]. The yearly  $^{14}\text{C}$  events count for a 10 tons fiducial volume of the proposed detector are tabulated in table 3. The count from the other background sources are presented in the same table.

### 6.2.2 $^{14}\text{C}$ spectrum and the detector's threshold

In order to separate events from the background on the  $^{14}\text{C}$  spectrum tail it is necessary to acquire the part of the spectrum under the physical threshold of the detector (170 keV). We propose to use the following technique for the detector triggering. First, the lower level trigger is produced as a coincidence of the signals from 20 PMTs in the 50 ns gate. This will give a random coincidence rate at the level  $< 10^{-10}$  ev/year if all the PMTs have a dark rate less than 5 kHz. The high level trigger is produced if the total collected charge is greater than the preset threshold  $Q_{th}$ . The choice of this threshold will be defined by the resolution of the

detector. Let us estimate the last quantity. The mean number of channels fired for the event with an energy  $E$  at the detector's center is:

$$\langle N \rangle = N_{PM}(1 - e^{-\mu_0}), \quad (6)$$

where  $\mu_0$  is the mean number of photoelectrons registered by one PMT in the event and  $N_{PM} = 800$  is the number of the PMTs of the detector. The solution of (6) for  $\langle N \rangle = 20$  will yield  $\mu_0 \simeq 0.025$ , i.e. a total collected charge of 20 p.e. This value is the detector threshold in the sense that only 50% of the events with an energy corresponding to this charge are registered. Of course, this causes a significant spectrum deformation near the threshold. In order to avoid these deformations one should set the threshold at the level that will cut the events with energies that are not providing 100% registration, i.e.  $Q_{th} + 3\sigma_{Q_{th}} = 20 + 3\sqrt{20} = 33.4$  p.e. This charge corresponds to approximately 35 keV if the ionization quenching at this energy is 50%. Though the calculation was performed for the event at the detector's center and the real situation is complicated by the electronics threshold, it gives the value very close to the one obtained with Monte Carlo simulation.

### 6.2.3 $^{14}C$ pile-up events

A potential danger are the  $^{14}C$  pile-up events, i.e. events occurring sequentially within a coincidence window. Such event can in principle influence the  $^{14}C$  spectrum tail, as one can see in fig.3. The fraction of the  $^{14}C$  pile-up events with energies above 170 keV is about 5%. The total amount of pile-up events depends on the  $^{14}C$  relative abundance and on the coincidence window:

$$N_{p.u.} = \tau_{Gate} \times f_{^{14}C}^2 \times T, \quad (7)$$

where  $T$  is the total time of the data taking,  $\tau_{Gate} = 60$  ns is the coincidence gate width, and  $f_{^{14}C}$  is the frequency of the  $^{14}C$  events. For a  $^{14}C$  abundance of  $2 \times 10^{-18}$  g/g, the mean rate of the events caused by  $^{14}C$  beta- decay is 2.2Hz. With these values the number of pile-up events is 2.5 per day, and the number of events with energy greater then 170 keV is only about 0.13 per day.

The excellent spatial resolution of the detector provides a further possibility to suppress the amount of these events by a factor of at least  $\left(\frac{\frac{4}{3}\pi(3\sigma_R)^3}{V_{FV}}\right)^2 = \left(\frac{3\sigma_R}{R_{FV}}\right)^6 \simeq 10^{-5}$ , where  $\sigma_R$  is the spatial resolution at 170keV and  $R_{FV} = 140$ cm is the radius of

E [keV]	$^{14}\text{C}$	Int.bkg.	$\sqrt{bkg}$	pp	$^7\text{Be}$	$\nu$ -s tot
148.4	73291.8	6.8	270.7	74.6	13.7	93.3
151.6	49755.8	6.7	223.1	71.7	13.7	90.4
154.8	32443.6	6.7	180.1	68.9	13.7	87.5
158.1	20254.8	6.6	142.3	66.0	13.7	84.6
161.3	12070.3	6.5	109.9	63.2	13.6	81.8
164.5	6846.4	6.4	82.8	60.4	13.6	78.9
167.7	3686.5	6.4	60.8	57.6	13.6	76.1
170.9	1879.8	6.3	43.4	54.7	13.6	73.2
174.1	905.8	6.2	30.2	52.0	13.6	70.4
177.3	411.6	6.2	20.4	49.2	13.6	67.6
180.6	176.1	6.1	13.5	46.4	13.5	64.8
183.8	70.8	6.0	8.8	43.7	13.5	62.1
187.0	26.7	6.0	5.7	41.1	13.5	59.4
190.2	9.4	5.9	3.9	38.5	13.5	56.8
193.4	3.1	5.9	3.0	35.9	13.5	54.2
196.6	1.0	5.8	2.6	33.4	13.5	51.7
199.8	0.3	5.7	2.5	31.0	13.5	49.2
203.0	0.1	5.7	2.4	28.7	13.4	46.9
206.2	0.0	5.6	2.4	26.4	13.4	44.5
209.4	0.0	5.6	2.4	24.2	13.4	42.2
212.7	0.0	5.5	2.3	22.0	13.4	40.0
215.9	0.0	5.5	2.3	19.9	13.4	37.7
219.1	0.0	5.4	2.3	17.8	13.4	35.6
222.3	0.0	5.3	2.3	15.8	13.4	33.4
225.5	0.0	5.3	2.3	13.9	13.3	31.3
228.7	0.0	5.2	2.3	12.1	13.3	29.3
231.9	0.0	5.2	2.3	10.4	13.3	27.5
235.1	0.0	5.1	2.3	8.8	13.3	25.7
238.3	0.0	5.1	2.3	7.3	13.3	24.1
241.5	0.0	5.0	2.2	5.9	13.3	22.6
244.7	0.0	5.0	2.2	4.7	13.3	21.4
247.9	0.0	4.9	2.2	3.6	13.3	20.3

Table 3:  $^{14}\text{C}$  events count and other internal background sources events in the 10 tons fiducial volume of the proposed upgrade of the CTF detector (for 1 year of the data taking). The expected effect for the pp, $^7\text{Be}$  and total neutrinos count in the SSM is presented for comparison.

the fiducial volume. Thus, one can conclude that pile-up events are not influencing the shape of the  $^{14}\text{C}$  spectrum within the considered energy interval.

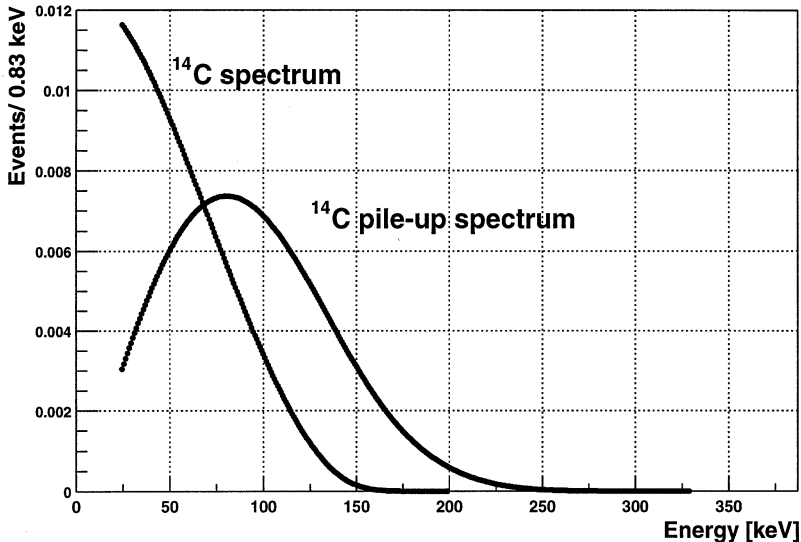


Figure 3: Pile-up events spectrum in comparison to the  $^{14}\text{C}$  spectrum.

### 6.3 Background from the radon in the water buffer

This background is expected to be efficiently rejected by the radial cut. The special nylon shroud tested with the CTF-II setup should prevent the diffusion of the external radon into the scintillator volume, reducing the background observed in CTF by a factor of 10 to 1000.

The raw count observed in CTF-I was  $0.3 \frac{ev}{kg \cdot keV \cdot year}$  in the 250-800 keV energy window, in CTF-II it was about  $0.1 \frac{ev}{kg \cdot keV \cdot year}$ . But in the latter case this background was dominated by the  $^{40}\text{K}$  contained in the strings supporting the inner vessel.

### 6.4 External gamma background

The background count, caused mainly by the radioactive contamination of the PMT glass with  $^{40}\text{K}$  and the elements of the U-Th chain, has been evaluated with an EGS4 code. We include in the MC simulation the ionization quenching effect [22] and the limited spatial reconstruction ability at the lower energies. The assumed

content of the  $^{238}\text{U}$ ,  $^{232}\text{Th}$  and  $K_{nat}$  in the PMTs is  $112.4 \mu\text{g}/\text{PMT}$ ,  $47.3 \mu\text{g}/\text{PMT}$  and  $62.3 \text{mg}/\text{PMT}$  respectively, which corresponds to the measured radioactive contamination of the phototubes produced with high purity glass. We add 30% to these values to account for the radioactive contamination of the concentrator and PMT divider, sealing and support structure.

The results of simulation are presented in fig.4. One can see that  $R < 150$  cm spatial cut will eliminate all the events in the neutrino window (170-250 keV).

In order to reduce the background from the penetrating gamma's we suggest to reduce the amount of the construction materials contributing to the background. A significant amount of the material in Borexino is contained in the mu-metal shield of the PMTs, which is providing the screening of the PMTs against the terrestrial magnetic field. Alternative solution based on the PMTs orientation has been studied in [19]. The effect of the PMTs orientation is comparable to the one achieved with the PMT screening with the metal with high magnetic permeability. Use of this technique could eliminate about 1 kg of material for each PMT in proximity to the inner vessel.

Another possibility to reduce the gamma background is assuming the use of a different topology of the events produced by electrons and gammas. The excellent spatial resolution of the CTF upgrade will permit distinguishing point-like energy deposits for electrons from the distributed gamma events ( $\beta/\gamma$  discrimination). The study of the possibility of such discrimination for the Borexino detector is now in progress.

## 6.5 Cosmic ray induced background

The cosmic ray induced background can be subdivided into the tree categories:

1. Muons crossing the water buffer of the detector, producing the Cerenkov light;
2. Neutrons produced by muon interactions, and sequentially stopped in the water or scintillator and emitting 2.2 MeV annihilation gamma;
3. Secondary radioactive nuclei produced in the muon interactions inside the detector.

Most of the background counts associated with muons can be effectively removed by the muon identifying system (muon veto). One can use the time and spatial

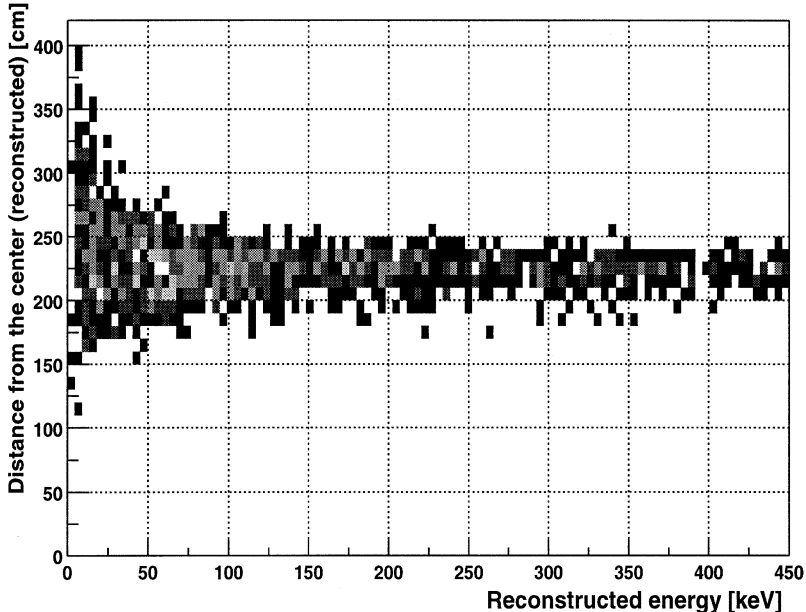


Figure 4: External gammas background simulation in the energy window up to 450 keV (1 day). One can see that  $R < 150$  cm spatial cut will eliminate all the events in the pp- neutrino window (170-250 keV).

structure of the muon induced events in order to recognize them. The muon identification procedure was able to recognize 95% of the muon induced events in the CTF-I detector [13]. We assume also the use of a set of the PMTs situated on the top and bottom of the cylindrical external tank that will increase the muon identification to a value approaching 100%.

Some of the radioactive products of the muon interactions with the scintillator have significant life time, that makes impossible the use if the muon tag. These isotopes are  $^{11}\text{Be}$  ( $\beta^-$ , 11.5 MeV, 13.8 s),  $^{10}\text{C}$  ( $\beta^+$ , 1.9 MeV +  $\gamma$ , 0.72 MeV, 19.3 s),  $^{11}\text{C}$  ( $\beta^+$ , 0.99 MeV, 20.38 min) and  $^7\text{Be}$  ( $\gamma$ , 0.478 MeV, 53.3 days). The considered neutrino window is too narrow to pick up significant amount of the events from these isotopes. The precise evaluations are now in progress for the Borexino detector, but this background will certainly will be negligible in comparison to the other sources considered.



## 6.6 $^{14}\text{C}$ content. Is it critical?

It is commonly assumed that  $^{14}\text{C}$  content is setting the limit on sensitivity at the low energy region in the liquid organic scintillator. The ratio as low as  $2 \times 10^{-18}$  g/g was achieved with CTF detector. There are indications that content of  $^{14}\text{C}$  can be even smaller, of the order of  $10^{-21}$  g/g [23]<sup>3</sup>. In this case the  $^{14}\text{C}$  contribution in the background can be reduced by the factor 2000. It is interesting to study the sensitivity of the detector to the pp- neutrinos in dependence on the content of the  $^{14}\text{C}$  in the scintillator. The results of the study are summarized in table 4. One can see that the detector sensitivity is varying rather slowly with the decrease of the  $^{14}\text{C}$  content in the scintillator. There are several reasons for this behaviour. First of all, the pp neutrinos rate is quite low and with minimal background contribution the statistical fluctuations of the pp rate are the major source of the uncertainty. Another source of uncertainty is the irreducible internal background which becomes comparable to the  $^{14}\text{C}$  events contribution at the lower  $^{14}\text{C}$  content. The last reason is the lower threshold of the detector of about 25 keV, which can't be decreased without picking up the random electronics noise. In order to avoid the influence of the threshold effect on the signal shape it is necessary to set software threshold even higher, about 40 keV. Another reason to set a higher software threshold is the presence of low energy external gammas which can be reconstructed inside the fiducial volume due to the poor spatial resolution at low energies.

We can conclude that lower  $^{14}\text{C}$  would be desirable but is not critical for the detector sensitivity to the pp- neutrinos.

## 7 Neutrino signals

In the calculations we used SSM fluxes given by the standard solar model[24], neutrino energy spectra from [25]-[27] and survival probabilities for the different solar neutrino scenarios from [28]. Signal shapes were convolved with the detectors response function using (3).

---

<sup>3</sup>New petro-geological model allows such a low value, contamination with modern  $^{14}\text{C}$  in this case have to be excluded during petroleum refinement [23]. The existing CTF setup is suitable device for the search of the organic LS with minimal  $^{14}\text{C}$  contamination.

$^{14}\text{C}$ [g/g]	$2 \times 10^{-18}$	$10^{-19}$	$10^{-20}$	$10^{-21}$
threshold ( $\sqrt{bkg}=\text{eff}$ )	174 (40)	145	0	0
threshold ( $2\sqrt{bkg}=\text{eff}$ )	182	156	125	0
energy interval	170-250	160-250	150-250	150-250
$^{14}\text{C}$ events	3485	1304	643	64
Int.Bkg (Borexino)	140	159	180	180
pp	647	829	1035	1035
total $\nu$ 's	1092	1329	1591	1591
fit region	40-330	40-330	40-330	40-330
uncertainty (1 $\sigma$ c.l.),fit	0.056	0.05	0.04	0.034

Table 4: The sensitivity of the detector to the SSM pp- neutrinos in dependence on the content of the  $^{14}\text{C}$  in the scintillator.

## 7.1 Sensitivity to the pp-neutrinos

The pp-neutrino count in different solar neutrino oscillation scenarios are listed in table 5. The sensitivity was estimated with the Monte- Carlo method. First, the total signal was calculated taking into account the detector's resolution. In the next step the normally distributed random signal was generated at each bin.

A fitting function consists of the function describing the internal background (without  $^{14}\text{C}$ ), the spectrum of the  $^{14}\text{C}$  decay and the neutrino signal:

$$f(q) = N_{Bkg}Bkg(q) + N_{^{14}\text{C}} \cdot C(q) + N_{\nu}\phi_{\nu}(q). \quad (8)$$

The shape of the internal background Bkg(q) was fixed, but its normalization ( $N_{Bkg}$ ) was free. Another free parameter is normalization of the  $^{14}\text{C}$  spectrum  $N_{^{14}\text{C}}$ .

The rates listed in table 5 are calculated in the energy window 170-250 keV taking into account detector's resolution. The neutral current channel for the neutrinos of non- electron flavours are taken into account in the calculations. Other neutrino sources also have non- negligible contributions to the total signal in this energy window. The main source besides the pp are  $^7\text{Be}$  neutrinos with a flat spectrum (see fig.5).

The uncertainty of the total neutrino flux measurement are given in the table.5 for the case of the internal background at the level envisaged for the Borexino and for a 10 times bigger background. For convenience, the uncertainties are measured in the units of the corresponding model flux. The possible systematics errors because of the unknown shape of the background are not included in the estimation. We

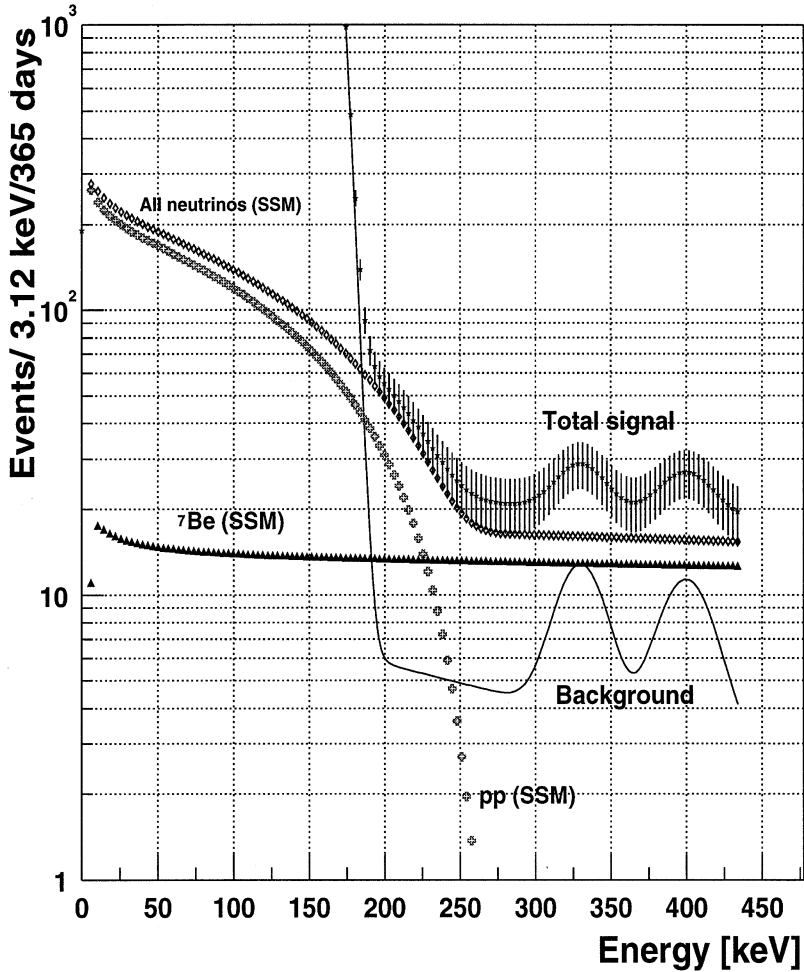


Figure 5: Signal and background shape for the SSM neutrino fluxes.  ${}^{14}\text{C}$  content is  $2 \times 10^{-18} \text{g/g}$ . Other background components are considered to be the same as Borexino background. Detectors mass is 10 tons. The resolution is calculated in the assumption of 100% geometrical coverage using CTF-I light output (i.e. 1800 p.e./MeV) and is assumed to be  $\frac{1}{\sqrt{N_{\text{p.e.}}}}$ . Shown signals correspond to 1 year of the data taking.

counts/year [170-250 keV]	SSM	SMA	LMA	LOW	LOW (Day)	LOW (Night)
pp	647	434	424	414	342	488
total $\nu$ 's	1092	535	676	673	570	776
$^{14}\text{C}$ [ $2 \cdot 10^{-18} \text{ g/g}$ ]	3485					
Int.Bkg (Borexino)	140					
uncertainty ( $1\sigma$ c.l.), fit [40-330 keV]	0.056	0.077	0.074	0.07	0.085	0.068
Int.Bkg (10xBorexino)	1400					
uncertainty ( $1\sigma$ c.l.), fit [40-330 keV]	0.09	0.13	0.13	0.13	0.15	0.11

Table 5: The pp-neutrino count in different solar neutrino oscillation scenarios.

assume that MC simulation can reproduce the form of the background and only the total normalization of this shape is unknown. The assumption is reasonable because of the quite narrow signal window, where the background is dominated by the slowly varying continuous spectrum of the soft part of the gamma spectra of radioactive impurities.

## 7.2 Discrimination ability in respect to the various solar neutrino scenarios

In order to investigate the sensitivity of the set-up to the different neutrino oscillation scenarios we performed a fit of the MC simulated data with the neutrino fluxes in all scenarios. The results are summed in table 6. The columns represents the model used for the MC simulation, while in the rows are presented the results of the fit applied using different scenarios. For each fit we give the total normalization of the flux  $N_\phi$  (in the units of the corresponding scenario flux), the flux uncertainty at  $1\sigma$  c.l., measured in the units of the model used for the fit flux, and the  $\chi^2$  value (80 d.o.f.)

One can see that SMA solution is well discriminated from the others both by the count and by the shape. LMA and LOW are indistinguishable, but the LOW solution has a significant day/night variation.

	SSM			SMA			LMA			LOW		
	$N_\phi$	$\sigma$	$\chi^2$	$N_\phi$	$\sigma$	$\chi^2$	$N_\phi$	$\sigma$	$\chi^2$	$N_\phi$	$\sigma$	$\chi^2$
SSM	1.02	0.06	72.8	0.53	0.04	85.3	0.66	0.08	72.9	0.64	0.05	72.4
SMA	1.96	0.08	115.1	1.01	0.08	71.0	1.05	0.13	76.3	1.10	0.08	85.2
LMA	1.62	0.09	74.7	0.85	0.07	81.4	1.03	0.13	73.3	1.00	0.08	72.9
LOW	1.64	0.09	74.0	0.85	0.07	82.4	1.05	0.13	73.2	1.02	0.08	72.7

Table 6: The discrimination between different neutrino oscillation scenarios.

### 7.3 Sensitivity to ${}^7\text{Be}$ neutrinos

The detector will count 1840  ${}^7\text{Be}$  SSM neutrinos per year in the 200-700 keV energy window with the internal background of 736 event. For comparison Borexino detector will count 16152 events in the 250-750 keV energy window with the background of 6468 events. We are not presenting here the evaluation of the sensitivity of the detector to the  ${}^7\text{Be}$  neutrinos. It is clear that the lower mass (factor 10) with comparison to the Borexino detector will limit the sensitivity. The certain gain in the sensitivity can be achieved due to the better energy resolution of the detector (factor 2.1). The sensitivity relative to Borexino for equal time of data taking and equal specific background can be estimated as  $\sqrt{\frac{M_{Det} \sigma_{Borex}}{M_{Borex} \sigma_{Det}}} \simeq 0.45$ . In fig.6 and 7 the signal shape for the both detectors is presented.

## 8 Improvement of the detector performances

The performance of the detector can be improved by using any of the following ideas:

1. **Use of the specially designed photomultipliers, providing better quantum efficiency.** The basic idea is the ‘‘recycling’’ of the incoming photons. Various optical arrangements have been used to improve light absorption by letting incoming light interact with the photocathode material more than once (see i.e. [33]). The idea is revived in the recent works [34],[35], where authors reported significant increase of the quantum efficiency, up to the factor 2.
2. **Use of the beta/gamma discrimination techniques.** The usage of the different topology of the point-like beta events and the spatially distributed gamma- events can provide the opportunity to discriminate between beta and

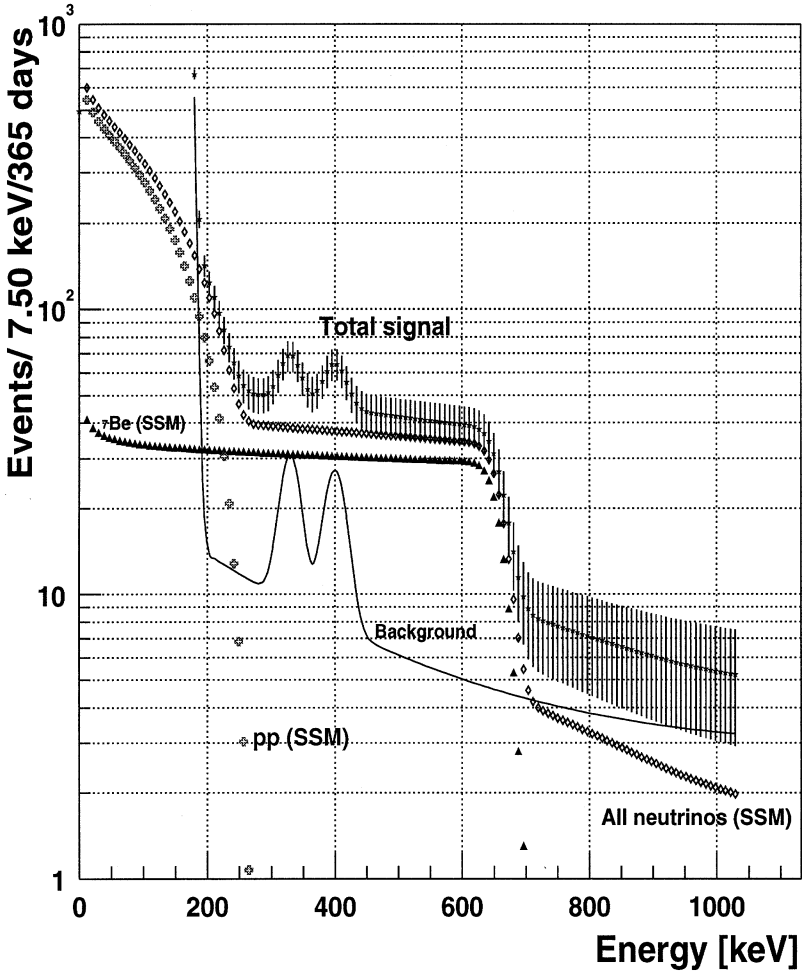


Figure 6: CTF upgrade. Signal and background shape for the SSM neutrino fluxes.  $^{14}\text{C}$  content is  $2 \times 10^{-18} \text{ g/g}$ . Other background components are considered to be the same as Borexino background. Detectors mass is 10 tons. The resolution is calculated in the assumption of 100% geometrical coverage using CTF-I light output (i.e. 1800 p.e./MeV) and is assumed to be  $\frac{1}{\sqrt{N_{p.e.}}}$ . Shown signals correspond to 1 year of the data taking.

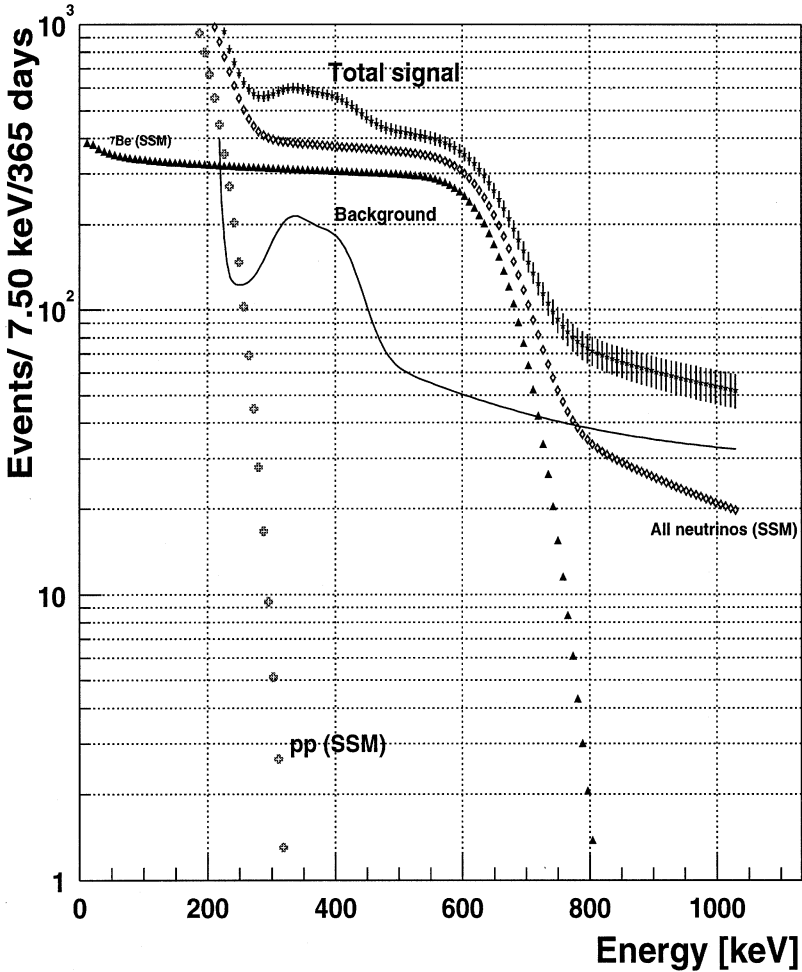


Figure 7: Borexino. Signal and background shape for the SSM neutrino fluxes.  $^{14}\text{C}$  content is  $2 \times 10^{-18}\text{g/g}$ . Detectors mass is 100 tons. The resolution is calculated using 400 p.e./MeV light output and is assumed to be  $\frac{1}{\sqrt{N_{p.e.}}}$ . Shown signals correspond to 1 year of the data taking.

gamma induced signals with high efficiency. The method is exploiting the superior resolutions of the detector.

3. **Choice of the organic scintillator with lower content of  $^{14}\text{C}$ .** There are indications that content of  $^{14}\text{C}$  can be much smaller than measured with the CTF-I detector, namely of the order of  $10^{-21}$  g/g [23]. In this case the  $^{14}\text{C}$  contribution in the background can be significantly reduced, that will lead to the improvement of the detector's characteristics.

## 9 Conclusions

The following upgrade of the CTF detector is considered:

- geometrical coverage of 100%, providing light yield of 1800 p.e./1 MeV;
- inner vessel radius 240 cm (50 tons of PC) ;
- active shielding of the active volume with 1 meter of pseudocumene;
- the distance from the PMTs photocathode to the detectors center is 4.3 m.

The project can compete with other existing proposals (see table 1). At the same time the proposed detector, being based on the technologies already developed for the Borexino project, is more realistic.

The further improvement of the detector performances can be achieved using techniques mentioned in section 8.

## Acknowledgements

This job would have been impossible without the support from the INFN sez. di Milano. We would like to thank Prof. G.Bellini and Dr. G.Ranucci who organized the stay of two of us at the LNGS laboratory during the summer 2001, as well as the LNGS personal for their friendliness.

We would like to thank all the colleagues from the Borexino collaboration for the pleasure to work together. Special thanks to R.Ford for the careful reading of the manuscript.



## References

- [1] E.Calabresu, G.Fiorentini, and M.Lissia. "Physics potential of pp and pep solar neutrino fluxes". astro-ph/9602045, 1996.
- [2] J.N.Bahcall. "Why do solar neutrino experiments below 1 MeV?". Proc.Second International Workshop on Low Energy Solar Neutrinos, University of Tokyo, Japan. 2000.
- [3] R.S.Raghavan. "Real time spectroscopy of pp and Be solar electron- neutrinos by LENS." LENS meeting at LNGS, Assergi, 28-th July 1998.  
M.Fujiwara et al. arXiv:nucl-ex/0006006, 2000.
- [4] R.S.Raghavan. "pp-Solar Neutrino Spectroscopy: Return of the Indium Detector." Bell Labs Tech.Memo. 10009622-010606-19TM.
- [5] H.V.Klapdor-Kleingrothaus. "GENIUS- A New Facility of Non-Accelerator Particle Physics." Nucl. Phys. B (Proc.Suppl.) 100 (2001) 350-355.
- [6] H.Ejiri. "Molibdenum observatory of neutrinos." Proc. Int. Workshop on Low Energy Solar Neutrinos, LowNu2, December 4 and 5 (2000) Tokyo, Japan, ed: Y.Suzuki, World Scientific, Singapore (2001), home page: <http://www-sk.icrr.u-tokyo.ac.jp/neutlowe/2/transparency/index.html>
- [7] The HERON project. By R.E. Lanou (Brown U.). 1999. In "Venice 1999, Neutrino telescopes, vol. 1" 139-146.
- [8] C.Broggini. "NUMU as a solar neutrino detector." Proc. Int. Workshop on Low Energy Solar Neutrinos, LowNu2, December 4 and 5 (2000) Tokyo, Japan, ed: Y.Suzuki, World Scientific, Singapore (2001), home page: <http://www-sk.icrr.u-tokyo.ac.jp/neutlowe/2/transparency/index.html>
- [9] Y.Suzuki for the XMASS collaboration. "Low energy solar neutrino detection using liquid xenon." Proc. Int. Workshop on Low Energy Solar Neutrinos, LowNu2, December 4 and 5 (2000) Tokyo, Japan, ed: Y.Suzuki, World Scientific, Singapore (2001), home page: <http://www-sk.icrr.u-tokyo.ac.jp/neutlowe/2/transparency/index.html>  
Y.Suzuki for the Xenon collaboration. "Low energy solar neutrino detection by using liquid xenon". hep-ph/0008296, 2000.

- [10] A.Sarrat on behalf of the HELLAZ collaboration. "HELLAZ: a low energy neutrino spectrometer." Nucl. Phys. B (Proc.Suppl.) 95 (2001) 177-180.
- [11] D.N. McKinsey, J.M. Doyle. "Liquid Helium and liquid neon: sensitive low background scintillation media for the detection of low energy neutrinos." astro-ph/9907314, 1999.
- [12] Arpesella C. et al, Borexino at Gran Sasso - Proposal for a real time detector for low energy solar neutrino.. Volume 1. Edited by G.Bellini,M.Campanella,D.Guigni. Dept. of Physics of the University of Milano. August 1991.
- [13] Alimonti G. et al "A large scale low-background liquid scintillator detector: the counting test facility at Gran Sasso". NIM A 406 (1998) p.411-426
- [14] Alimonti G. et al. "Light propagation in a large volume liquid scintillator." NIM A440 (1998) 360.
- [15] Alimonti G. et al. " Ultra-low Background Measurements in a large volume underground experiment." Astroparticle Physics 8(1998) 141-157.
- [16] Alimonti G. et al. "Measurement of the  $^{14}\text{C}$  abundance in a low-background liquid scintillator." Phys.Lett. B 422 (1998) 349-358.
- [17] Alimonti G. et al. " Science and technology of Borexino: a real time detector for low energy solar neutrinos", Accepted by Astroparticle Physics, 2001.
- [18] G.Ranucci et al., Nucl.Instr.Meth. A333 (1993) 553
- [19] A. Ianni, G. Korga, G. Ranucci, O. Smirnov, A. Sotnikov. "Compensating the influence of the Earth's Magnetic Field on the scintillator detector resolutions by PMTs orientation." LNGS preprint INFN/TC-00/05, 2000.
- [20] O.Smirnov. "Resolutions of a large volume liquid scintillator detector." LNGS preprint INFN/TC-00/08, 2000.
- [21] O.Smirnov. "Energy reconstruction in a large volume liquid scintillator detector." in preparation.

- [22] S.Bonetti, O.Donghi, C.Salvo, G.Testera. "Ionization quenching: effects on  $e^-$  and  $\gamma$  detection in Borexino and in CTF". Borexino internal report 98/10/15, 1998.
- [23] E. Resconi, "Measurements with the Upgraded Counting Test Facility (CTF-2) of the Solar Neutrino Experiment Borexino", Doctorate Thesis, Universita' degli Studi di Genova, 2001  
S.Schoenert. Private communication.
- [24] J. N. Bahcall, H. Pinsonneault, and Sarbani Basu, astro-ph/0010346, 2000.
- [25] J. N. Bahcall and R. K. Ulrich, Rev. Mod. Phys. 60, 297 (1988)
- [26] J.N. Bahcall, E. Lisi, D.E. Alburger, L. De Braeckelee, S.J. Freedman, and J. Napolitano, Phys. Rev. C., 54, 411-422.
- [27] J.N. Bahcall, Phys. Rev. C. 56 3391(1997).
- [28] J.N. Bahcall, Krastev, and A.Ju.Smirnov, Phys. Rev. D, 58, 096016 (1998).
- [29] M.Morita, Beta Decay and Muon Capture, Benjamin, Reading, Mass., (1973)  
33
- [30] J.J.Simpson, A.Hime, Phys.Rev. 39D (1989) 1825
- [31] H.Behrens, J.Janecke, Numerical Tables for beta-decay and electron capture, ed. H.Schopper, Landolt-Bornstein, Springer, Berlin, 4 (1969)
- [32] M.E.Rose, Phys.Rev. 49 (1936) 727
- [33] W.D.Gunter, Jr., G.R.Grant, and S.A.Shaw. "Optical devices to increase photocathode efficiency." Appl.Optics. Vol. 9, No.2 (1970) 251.
- [34] S.Harmer, S.Hallensleben, P.D.Townsend. "Realisation of 50% quantum efficiency from photomultiplier cathodes". NIM B, 166-167(2000) 798-803.
- [35] S.Hallensleben, S.Harmer, P.D.Townsend. "Optical constants for the S20 photocathode, and their application to increasing photomultiplier quantum efficiency". Optics Comm. 180(2000)89-102.

---

Received by Publishing Department  
on September 7, 2001.

Смирнов О.Ю., Займидорога О.А., Дербин А.В.  
Измерение потока солнечных  $pp$ -нейтрино  
на модифицированном детекторе CTF

E15-2001-188

Показана возможность регистрации низкоэнергетических солнечных нейтрино с помощью детектора на основе сверхчистого жидкого органического сцинтиллятора. Детектор с активным объемом 10 тонн может регистрировать 1,8  $pp$ -нейтрино и 5,4  ${}^7\text{Be}$ -нейтрино в сутки с порогом энергии 170 кэВ по электронам отдачи. Оценки радиоактивных фонов и чувствительности детектора основываются на результатах, полученных коллаборацией «Борексино» на детекторе CTF. Детектор может быть сооружен в подземной лаборатории Гран-Сассо (Италия) на базе существующей установки с использованием технологий, опробованных для детектора «Борексино».

Работа выполнена в Лаборатории физики частиц ОИЯИ и в Санкт-Петербургском институте ядерной физики, Гатчина.

Препринт Объединенного института ядерных исследований. Дубна, 2001

Smirnov O.Yu., Zaimidoroga O.A., Derbin A.V.  
Search for the Solar  $pp$ -Neutrinos with an Upgrade  
of CTF Detector

E15-2001-188

A possibility to use ultrapure liquid organic scintillator as a low energy solar neutrino detector is discussed. The detector with an active volume of 10 tons and  $4\pi$  coverage will count 1.8  $pp$ -neutrinos and 5.4  ${}^7\text{Be}$  neutrinos per day with an energy threshold of 170 keV for the recoil electrons. The evaluation of the detector sensitivity and backgrounds is based on the results obtained by the Borexino collaboration with the Counting Test Facility (CTF). The detector can be build at the Italian Gran Sasso underground laboratory as an upgrade of the CTF detector using already developed technologies.

The investigation has been performed at the Laboratory of Particle Physics, JINR and at the St. Petersburg Nuclear Physics Institute, Gatchina.

Preprint of the Joint Institute for Nuclear Research. Dubna, 2001

Макет Т.Е.Попеко

Подписано в печать 11.10.2001

Формат 60 × 90/16. Офсетная печать. Уч.-изд. л. 2,56

Тираж 280. Заказ 52894. Цена 3 р.

Издательский отдел Объединенного института ядерных исследований  
Дубна Московской области